

1 Dear Prof. Bruce Malamud,  
2

3 Please find enclosed the revised version of our manuscript entitled “Brief Communication: Rapid  
4 Mapping Of Event Landslides: The 3 December 2013 Montescaglioso Landslide (Italy)”. Firstly,  
5 thanks for your time and effort spent in dealing with our manuscript. We have found the criticism,  
6 comments, and suggestions received from you and the referees very constructive, and we have  
7 considered all of them in the revised version of our work. As you suggested, and in order to comply  
8 with the referee’s requirements, we have slightly exceeded the number of references allocated for Brief  
9 Communications (24 instead of 20).

10  
11 Please find here below for your reference the referee’s comments, and in **Bold** our replies. Changes in  
12 the manuscript text are highlighted in ***Bold Italic***.

13  
14 Looking forward to receiving the final acceptance of our manuscript,  
15

16 Sincerely yours.

17  
18 Andrea Manconi  
19 (Corresponding author)  
20  
21  
22  
23  
24

25 Anonymous Referee #1

26 Received and published: 18 March 2014

27 Review of the manuscript “RAPID MAPPING OF EVENT LANDSLIDES: THE 3 DECEMBER  
28 2013 MONTESCAGLIOSO LANDSLIDE (ITALY)” by A. Manconi et al. MS

29 No.: nhess-2014-41  
30

31 The manuscript by Manconi and coauthor describes a slope failure in Italy that occurred on 3  
32 December 2013. The authors use a cross-correlation approach (if my guess is correct) applied to  
33 satellite radar data acquired by the Italian satellite CosmoSkymed. The Montescaglioso landslide was  
34 shown to move by as much as 30 m horizontally, with significant hazards associated. The authors  
35 discuss whether the landslide was associated with intense rainfall.

36 The data analysis done on the radar data is certainly excellent, showing a spectacular event that  
37 occurred few months ago. The figures are high quality and all necessary (in fact also the figures in  
38 appendix are relevant). The writing, however, is rather poor and to my opinion misleading. Given the  
39 sound scientific analysis of the data and relevance of this particular landslide event, I can recommend  
40 the publication of the manuscript. Major major major rewriting has to be done, however, as detailed  
41 below.  
42

43 **Our reply: We thank the referee for the detailed comments and constructive criticism, as well as**  
44 **for recognizing the importance and the scientific sound of the data and of the analysis presented**  
45 **in our manuscript. Here below we will provide our replies to all the major and minor points**  
46 **raised, as well as details on how we considered the referee suggestions in the revised version of**

47 **the manuscript.**

48  
49  
50  
51  
52  
53  
54  
55  
56  
57  
58  
59  
60  
61  
62  
63  
64  
65  
66  
67  
68  
69  
70  
71  
72  
73  
74  
75  
76  
77  
78  
79  
80  
81  
82  
83  
84  
85  
86  
87  
88  
89  
90  
91  
92

Major points

1. Why the authors emphasize the “rapid” mapping and “rapid” analysis? This in fact was absolutely not clear. In the abstract alone, the word “rapid” can be found four times. Is a satellite imaging system that is acquiring every 16 days (the normal CosmosSkymed revisit period) so rapid? Other geophysical contributions dealing with rapid assessments after earthquakes and other hazards deal with timelines on the order of seconds or minutes. Here an analysis done weeks after a landslide hazard is not rapid. Please consider focusing on the geoscience contribution rather focusing on the “rapid” technique.

**Our reply: We thank the Referee #1 for this comment. We have now modified the abstract in order to avoid repetitions of the word “rapid”. The abstract now reads: “We present a new approach to measure 3-D surface deformations caused by a large, rapid moving landslide, in an emergency scenario. The technique exploits the amplitude information of high spatial and temporal resolution SAR images captured by the COSMO-SkyMed satellites. Here we show the results obtained for the Montescaglioso landslide, southern Italy. Displacements have dominant planimetric SSW component, and exceed 10 meters among large part of the landslide deposit. Slope failure damaged a main road, private homes, and commercial buildings. Our results open to the possibility of preparing 3-D surface deformation maps shortly after the occurrence of large landslides. ”**

We would like to remark that the main focus of our Brief Communication is indeed the assessment of 3-dimensional displacements shortly after an event landslide, and we intend to keep this focus. We think that mapping of 3-dimensional displacements shortly after an event by exploiting remote sensing techniques, and confirming the outcomes from such an analysis with those from field mapping, is a rather new concept in the context of landslide hazard, and to our knowledge this is the first example of successful application in an emergency scenario to support civil protection activities. We agree with the Referee #1 that in other contexts, such as earthquake hazard scenarios, the concept of “rapid” assessment is related to shorter timelines (minutes, or even seconds). But, in earthquake scenarios, these timelines are not referred to surface deformation mapping and/or assessment. To measure accurate 3-dimensional displacements relevant to earthquake scenarios in timelines of seconds or minutes, recent studies have shown that dense monitoring networks of continuous GPS stations might be a possibility in some areas, where location and extension of the potential seismogenic sources are known, and thus the GPS network might be installed in advance. This option is clearly unfeasible for event landslide scenarios, where location and extension of the phenomenon are usually unknown before the event occurrence.

93 2. The literature review in the introductions is flawed and needs to be rewritten. For instance, in line 20  
94 and following: Obviously the authors are not aware of the current alternative methods applied to  
95 satellite and ground imaging data, such as image cross-correlation, DEM differencing, and others.  
96 Please also consult the numerous publications that have emerged following the earthquake induced  
97 landslides in Japan following the Tohoku disaster, many of the studies are published and referred to in  
98 a book (Earthquake-Induced Landslides: Proceedings of the International Symposium on ... by Keizo  
99 Ugai et al, Springer 2013). Also consider ground based InSAR systems (Corsini et al., 2006 and  
100 Jaboyedoff et al., 2010), determination of the average spatial shift by a cross-correlation function image  
101 pairs (White et al., 2003), Target Detection and Tracking (Veeraraghavan et al., 2006) and others. A  
102 recent paper published by Gance and coauthors (Engineering Geology Volume 172, 8 April 2014,  
103 Pages 26–40) will allow to get some overview on the current photogrammetric methods.  
104

105 **Our reply: We thank the Referee #1 for providing additional literature information, mainly on**  
106 **the analysis of optical images in landslide scenarios. As remarked by the Editor, the manuscript**  
107 **is intended for a Brief Communication, thus an in-depth literature review would be**  
108 **inappropriate. We would like to remark that we are well aware of the great advances performed**  
109 **in the last years on methods for the identification, measurement, and analysis of displacements**  
110 **based on image processing. However, most of the techniques mentioned by the Referee #1 are**  
111 **more relevant in a context where “monitoring” of surface displacements of an instable slope is**  
112 **necessary, and thus not completely relevant to our study. In our work, instead, we want to show**  
113 **how is possible to map and measure displacements of event landslides in areas that have not**  
114 **shown significant signs of instability before. High-resolution terrestrial photogrammetry**  
115 **methods (Gance et al., 2014) can be well applied only at locations where the instability has been**  
116 **already identified, and the monitoring network deployed. The same applies to other ground**  
117 **based monitoring systems, such as GB-InSAR or Terrestrial LiDAR.**  
118

119 **Moreover, it is worth to remind that the quantitative exploitation of airborne and space-borne**  
120 **optical imagery with pixel-offset, target detection and tracking, etc., provide usually planimetric**  
121 **(2D) displacements, which in many cases are not sufficient for an accurate characterization of the**  
122 **landslide event, as well as to plan for monitoring and mitigation strategies in the event’s**  
123 **aftermath. The same concept has been highlighted in a recent publication: (Singleton et al., 2014,**  
124 **RSE, Volume 147, 5 May 2014, Pages 133–144) “However, optical images can only be used to assess**  
125 **purely horizontal movements (north–south and east–west directions) without consideration of the**  
126 **vertical component.” In addition, as mentioned in our Section 6, the use of optical imagery for**  
127 **rapid landslide mapping might be hindered by meteorological conditions: “the availability of**  
128 **exploitable data strictly depends on the meteorological conditions at the acquisition time, as for**  
129 **example cloud coverage might compromise the visibility of the area of interest.”**  
130

131 **Also, we are aware that DEM differencing based on the results of LiDAR surveys is an important**  
132 **tool to derive information on the topographic modifications due to landslides. However, in areas**  
133 **characterized by large planimetric motions (as the Montescaglioso landslide) the use of DEM**  
134 **differencing might result in misleading interpretations. Moreover, as we mentioned in Section 6:**  
135 **“Airborne LiDAR associated with photogrammetric surveys represent also a powerful remote**  
136 **sensing methodology to map post-event landslide deformation, as well as to estimate the mobilized**  
137 **mass volume (e.g., Giordan et al., 2013). Further, the acquisition of LiDAR data might be in some**  
138 **cases hampered by the high costs and operational issues, as well as by unsuitable meteorological**

139 *conditions in the event's aftermath.*"

140  
141  
142 3. Method is unclear. A section on methods is needed. Neither the PO method is detailed, nor the  
143 identification approach of fractures. How was the InSAR data processed. Detail the PO processing,  
144 which correlation term was used? Was it processed in the frequency domain? At which window and  
145 padding size? And so on.

146  
147 **Our reply:** We have added now more specifications on the method used. However, we remind  
148 that the method applied to the Montescaglioso case-study has been already detailed in Casu et al.,  
149 2011. The PO technique used is based on the Normalized Cross Correlation approach  
150 implemented in the AMPCOR subroutine, which is part of the ROI\_PAC code (Rosen et al.,  
151 2004). Specific details on the PO processing, such as the window size, were detailed in the caption  
152 of Figure 2: *"In particular, we exploited the AMPCOR Fortran routine available in the ROI\_PAC*  
153 *software (Rosen et al., 2004) using a matching window of 64×64 pixels. We calculated the PO*  
154 *considering a sparse grid with an under-sampling factor of four pixels. We applied a spatial*  
155 *smoothing filter to reduce high-frequency noise."* According also to the comments of the Referee  
156 #2, we have moved this section in the main text, in order to avoid misunderstandings. Since this  
157 paper is intended for a Brief Communication, we prefer to refer readers interested into more  
158 details on the processing approach to Casu et al, 2011, where the effect of different parameters  
159 relevant to the PO approach applied to SAR data are detailed and discussed extensively. The text  
160 now reads: *"Considering the poor quality of the DInSAR results, we applied the amplitude-based*  
161 *pixel-offset technique to the SAR data pairs across the event with the smallest spatial baselines, to*  
162 *reduce the impact of the spatial decorrelation. In particular, we considered the ascending 16*  
163 *January 2013 - 18 December 2013, and the descending 10 January 2013 - 12 December 2013 data*  
164 *pairs, characterized by spatial baselines of 155 m and 40 m, respectively, and covering approximately*  
165 *the same time interval. In particular, for these data pairs we exploited AMPCOR, a Fortran routine*  
166 *based on the Normalized Cross Correlation approach, and available in the ROI\_PAC software*  
167 *(Rosen et al., 2004). We considered a matching window of 64×64 pixels, and calculated the PO*  
168 *considering a sparse grid with an under-sampling factor of 4 pixels. We also applied a spatial*  
169 *smoothing filter to reduce high-frequency noise. Readers interested into more details of the PO*  
170 *processing used here are referred to (Casu et al., 2011)."*

171  
172 **As concerns the identification of fractures (and, actually, of all the other surface features**  
173 **produced by the landslide), this was carried out following the approach in Parise (2003), in turn**  
174 **deriving from a number of studies therein cited. A sentence has been added in the text to clarify**  
175 **this point.**

176  
177 4. Please add a chapter on the geologic interpretation. How rainfall and the landslide are related (if  
178 any)? Common concepts have to be discussed, associated to shear stress and pore pressure increase.

179  
180 **Our reply:** The geologic interpretation of the Montescaglioso landslide is beyond the scope of this  
181 paper. At the moment, several monitoring systems, as well as geological and geophysical  
182 investigations are ongoing. The results of these analyses are still preliminary, and will be the base  
183 of further research aimed at discussing the geological interpretation of this landslide event. The  
184 relationship between the event landslide and the rainfall, as well as the associated shear stress

185 **and eventual pore pressure increase are under investigation and will be the subject of further**  
186 **research.**

187

188

189 —

190 Minor points

191 —

192 1. Chapter 2, line 8: please add detail, how steep are the slopes. Facing which side? Is the configuration  
193 suited for your approach?

194

195 **Our reply: Mean slope in the landslide area is around 10%, mainly facing South-South-East. We**  
196 **added now this information in the revised manuscript. The slope configuration is well suitable for**  
197 **the approaches used, as demonstrated by the PO results obtained, which are well in agreement**  
198 **with the field observations.**

199

200 2. Chapter 2, line 10: please add a reference of the geological map authors/publisher

201 **Our reply: The reference has been added.**

202

203 3. Chapter 3, 1st paragraph: This is interesting but hard to read. Please restructure by first describing  
204 the earlier events. First discuss the October rain, second the December rain, third the landslide. Please  
205 also compare the rainfall to the seasonal rainfall, for instance: “in just 2 days a quarter of the annual  
206 rainfall was recorded”

207

208 **Our reply: We thank the reviewer for this comment. We better describe now the temporal**  
209 **evolution of the events. Moreover we compare the October and December rainfall to the mean**  
210 **seasonal and annual values, as suggested. The text now reads: “Between 5 and 8 October 2013, the**  
211 **general area between Apulia and Basilicata, including the town of Montescaglioso, was struck by a**  
212 **heavy rainfall event with a cumulated rainfall  $E = 246$  mm, and a mean rainfall intensity  $I = 3.6$**   
213 **mm·h<sup>-1</sup>. The event caused widespread flooding, numerous shallow landslides, severe economic**  
214 **losses, and four fatalities. Moreover, from 30 November (14:00 CET) to 2 December (22:00 CET),**  
215 **with a cumulated rainfall measured at the Ginosa rain gauge, located 8 km from Montescaglioso, of**  
216  **$E = 151.6$  mm, and mean rainfall intensity  $I = 2.7$  mm·h<sup>-1</sup>. The two events totalized about 70% of the**  
217 **mean annual rainfall concentrated in few days. ”**

218

219 4. Chapter 4, 1st paragraph. The analysis of the historical imagery would be worth to show in the paper  
220 or in the appendix. Figure S1 is only an interpretation of a data set that is not shown in the manuscript,  
221 analysed with a method that is not explained in the manuscript. At least the authors could create a  
222 composite map, using different images in different channels, to show the changes in a figure.

223

224 **Our reply: We thank the reviewer for this comment. In the revised version, we have better**  
225 **detailed the approach followed for the multitemporal inventory based on the interpretation of**  
226 **stereoscopic aerial photographs. In the Supplementary material, we added a table (S5) related to**  
227 **the aerial photographs used to produce the multitemporal inventory map.**

228

229 5. Figure S1 and S2 could go into the main text, including descriptions. The figure S2 shows the  
230 structural summary, that would be important to be compared to the displacement maps of figs 2 and 3.

231 Are any of the structures mapped active? Are any structures active, or does the PO method not have the  
232 resolution and sensitivity to localize such?

233

234 **Our reply: Figures in for the main text in NHESS Brief Communications are limited to 3. For**  
235 **this reason, also in the revised version of the manuscript we have kept Figure S1 and S2 in the**  
236 **supplementary information.**

237

238 6. Chapter 4, 2nd paragraph: photographs taken during helicopter flights: these are not provided,  
239 neither in the manuscript nor in the appendix. Figure S2 is not the one referred to in the text.

240

241 **Our reply: We thank the referee to point out the inconsistency. In the revised version, we have**  
242 **now included the Figure S6, relevant to a photograph taken form helicopter in the event's**  
243 **aftermath.**

244

245 7. Chapter 4, 2nd paragraph: How are the “geomorphological features” identified?

246

247 **Our reply: The geomorphological features were identified directly in the field, carrying out**  
248 **detailed surveys in the days immediately following the event. Many features were in fact canceled**  
249 **after 5 days, due to the need to create temporary roads for civil protection issues. The text has**  
250 **been slightly changed by adding a sentence to better explain the approach followed.**

251

252 8. Chapter 5, 2nd paragraph: How was the dInSAR data processed?

253

254 **Our reply: We have now added more details on the DInSAR processing. The text now reads “A**  
255 **first conventional DInSAR analysis was performed on the acquisitions across the investigated event,**  
256 **by following the approach detailed in Massonet et al., 1993. Moreover, spectral shift compensation**  
257 **and interferometric fringes filtering were carried out (Burgmann et al., 2000).”**

258

259 9. Chapter 5, 3rd paragraph: How was the PO processing set up? FFT? Window size? Oversampling?  
260 Masking? Correlation function? Multi pass? No words about these!

261

262 **Our reply: Please see also our reply to Major point 3**

263

264 10. Chapter 6, 1st paragraph: Completely change the scope. Omit the “rapid” discussion and focus  
265 more on the geoscientific results provided.

266

267 **Our reply: Please see our reply to Major point 1 and Major point 4.**

268

269 11. Chapter 6, 2nd paragraph: the sentence that “optical data can usually provide qualitative  
270 information only” is simply wrong, outdated and shows that the existing literature was not considered.

271

272 **Our reply: Please see our reply to Major point 2.**

273

274 Summary. I am aware that my comments are very critical. But the manuscript has many very valuable  
275 contents that are worth publishing. I hope my criticism help to reflect and improve this early stage  
276 manuscript.

277 Anonymous Referee #2  
278 Received and published: 26 March 2014

279  
280 Dear editor,  
281 Thank you for the opportunity to revise the paper titled "Brief communication: Rapid mapping of event  
282 landslides: the 3 December 2013 Montescaglioso landslide (Italy)". The main contribution of this work  
283 is the application of the pixel offset technique (PO) to measure 3D surface deformation of a large rapid  
284 moving landslide in an emergency situation (Montescaglioso, 3rd December 2013). The PO technique  
285 was used to exploit ascending and descending SAR image datasets captured by the COSMO-SkyMed.  
286 The 3-D ground deformation measurements confirmed the deformation mechanisms recognized and  
287 mapped through geomorphological and field mapping.  
288 This reviewer recognises the scientific value provided by this work and recommends its publication.  
289 Below you will find some minor comments aiming to improve the quality of the manuscript.

290  
291 **Our reply: We thank the Referee #2 for recognizing the scientific value provided by this work.**  
292 **Please find below our detailed answer to the minor comments provided.**

293  
294  
295 Minor comments:

296 Abstract: please consider to include retrieved results in terms of magnitude and direction of  
297 displacement measured with the proposed techniques/ approach. Note that measured displacements, up  
298 to 20 m, clearly overpass the detection thresholds of DInSAR techniques.

299  
300 **Our reply: We thank the Referee #2 for this comment. We have now included information on the**  
301 **results in the abstract, which now reads: “We present a new approach to measure 3-D surface**  
302 **deformations caused by a large, rapid moving landslide, in an emergency scenario. The technique**  
303 **exploits the amplitude information of high spatial and temporal resolution SAR images captured by**  
304 **the COSMO-SkyMed satellites. Here we show the results obtained for the Montescaglioso landslide,**  
305 **southern Italy. Displacements have dominant planimetric SSW component, and exceed 10 meters**  
306 **among large part of the landslide deposit. Slope failure damaged a main road, private homes, and**  
307 **commercial buildings. Our results open to the possibility of preparing 3-D surface deformation maps**  
308 **shortly after the occurrence of large landslides. ”**

309  
310  
311 Lines 10-12 page 1457: the authors comment about DInSAR limitations to measure rapid deformations  
312 but no references nor values are provided. I suggest quantifying DInSAR detection thresholds, which  
313 could be useful to compare them with the detection capacity of the PO technique. One way of doing  
314 this is to include some literature examples illustrating DInSAR detection limits for landslides  
315 (Wasowski et al.2014. Investigating landslides and unstable slopes with satellite Multi Temporal  
316 Interferometry: current issues and future perspectives. Engineering Geology; Strozzi et al.2013.  
317 Interpretation of aerial photographs and satellite SAR interferometry for the inventory of landslides."  
318 Remote Sensing). Note that standard DInSAR processing of ALOS PALSAR image has permitted to  
319 detect over to 1 m/yr in certain case studies (see García et al. 2013. DInSAR analysis of ALOS  
320 PALSAR images for the assessment of very slow landslides: the Tena Valley case study.Landslides.)

321  
322 **Our reply: We thank the referee for pointing out this issue. In the revised version of the**

323 **manuscript, we have now included some of the references suggested, in order to highlight the**  
324 **limitations and the detection thresholds of DInSAR. The text now reads:**

325  
326 **Section 1: “The main advantage of DInSAR is the possibility to measure sub-centimetric surface**  
327 **displacements over large areas ( $10^2$ - $10^5$  km<sup>2</sup>). However, in landslide scenarios DInSAR can be**  
328 **limited by the unsuitable exposure of the instable slope area with respect to the acquisition geometry,**  
329 **as well as by large and/or rapid displacements, which may overcome the maximum detectable**  
330 **surface velocities between consecutive SAR acquisitions (Wasowski and Bovenga, 2014). In the**  
331 **latter case, interferometric phase information may be affected by high fringe rates leading to**  
332 **processing difficulties in the phase unwrapping step, and/or to coherence loss due to misregistration**  
333 **errors (Casu et al., 2011).”**

334  
335 **Section 6: “When the slope exposure is suitable with the satellite acquisition geometry (Colesanti**  
336 **and Wasowski, 2006), space-borne SAR can be considered as a valid alternative to map and measure**  
337 **surface deformation relevant to landslide phenomena. This technique has the main advantage to**  
338 **acquire data day and night, as well as in any weather condition. In some particular case studies**  
339 **DInSAR processing of L-Band SAR imagery permitted to detect and measure landslide surface**  
340 **velocities up to 1 meter/year (Garcia et al., 2013). Though, as mentioned in the introduction, the**  
341 **exploitation of conventional DInSAR technique in large and catastrophic landslide scenarios is**  
342 **hindered by the very large and/or rapid deformation usually associated with this kind of events.”**

343  
344 Lines 21-24 page 1471: overall a larger explanation on how the PO and the 3D methods were applied  
345 would be useful. Information relevant to the PO technique and generation of the 3D surface  
346 deformation map is included in the captions of Figures 2 and 3 and not in the text. Please consider to  
347 extend the explanation on the manuscript of both the PO technique and the 3D approach.

348  
349 **Our reply: We thank the Referee #2 for this comment. As highlighted also by the Editor, the**  
350 **manuscript is intended for a Brief Communication, thus a detailed description of the herein used**  
351 **methodology is unsuitable. We refer the readers interested into more details on the PO technique**  
352 **to Casu et al., 2011, where the technique is extensively explained. Moreover, the approach used**  
353 **here to obtain the 3D displacements is straightforward, and well explained in Racoules et al.,**  
354 **2013 and Hu et al., 2014”**

355  
356 Line 25 page 1470: being a technique claimed to improve landslide event emergency management, I  
357 suggest to include the duration (days or hours) of the 3-D surface deformation technique from image  
358 acquisition to "real" or "potential" delivery to civil protection.

359  
360 **Our reply: We thank the Referee #2 for highlighting this point, which is the main focus of our**  
361 **contribution. We have now included this information in the revised version of the manuscript.**  
362 **The text now reads: “The application of the PO technique to get rapid assessment of surface**  
363 **displacements after an event depends on two main factors: (i) the availability of SAR imagery, which**  
364 **is constrained by the satellite configuration and predefined acquisition plan; (ii) the PO processing**  
365 **time to get 3-D deformation maps. Considering our case study, CSK imagery was available after 8**  
366 **and 15 days, for descending and ascending orbits, respectively. This was possible also because the**  
367 **CSK acquisition plan was modified specifically for the Montescaglioso emergency scenario. The 3-D**  
368 **deformation maps computed via the PO technique were ready to be delivered to the civil protection**



369 *authorities in less than 24 hours after receiving the SAR imagery. Depending on the area of interest*  
370 *and on the acquisition plan, CSK configuration may provide SAR images also with shorter revisit*  
371 *times. Thus, PO results can be potentially produced and delivered in timelines of few days after the*  
372 *event landslide.”*

373

374

375 Figure 1. Explain what D and E represent

376

377 **Our reply: Done, thanks for pointing out this inconsistency.**

378

379

380  
381

## *Brief Communication*

382 **RAPID MAPPING OF EVENT LANDSLIDES: THE 3 DECEMBER**  
383 **2013 MONTESCAGLIOSO LANDSLIDE, ITALY**

384

385 A. Manconi (\*)<sup>(1)</sup>, F. Casu <sup>(2)</sup>, F. Ardizzone <sup>(4)</sup>, M. Bonano <sup>(2)</sup>, M. Cardinali <sup>(4)</sup>, C. De Luca <sup>(2,3)</sup>, E.  
386 Gueguen <sup>(5)</sup>, I. Marchesini <sup>(4)</sup>, M. Parise <sup>(6)</sup>, C. Vennari <sup>(6)</sup>, R. Lanari <sup>(2)</sup>, F. Guzzetti <sup>(4)</sup>

387 <sup>(1)</sup> CNR IRPI, Strada delle Cacce 73, 10135, Torino, Italy

388 <sup>(2)</sup> CNR IREA, Via Diocleziano 328, 80124 Napoli, Italy

389 <sup>(3)</sup> Università degli Studi di Napoli Federico II, Via Claudio 21, 80124, Napoli

390 <sup>(4)</sup> CNR IRPI, Via della Madonna Alta 126, 06128 Perugia, Italy

391 <sup>(5)</sup> CNR IMAA, C.da Santa Loja, Tito Scalo, 85050 Potenza, Italy

392 <sup>(6)</sup> CNR IRPI, Via Amendola, 122/I, 70126 Bari, Italy

393

394 \*corresponding author, Email: [andrea.manconi@irpi.cnr.it](mailto:andrea.manconi@irpi.cnr.it), Phone: +39 011 3977 829, Fax: +39 011 3977 821

395

396

397

398 **Abstract**

399 We present an approach to measure 3D surface deformations caused by large, rapid moving landslides  
400 using the amplitude information of high resolution, X-band SAR images. We exploit SAR data  
401 captured by the COSMO-SkyMed satellites to measure the deformation produced by the 3 December  
402 2013 Montescaglioso landslide, southern Italy. The deformation produced by the deep-seated landslide  
403 exceeded 10 meters, and caused the disruption of a main road, a few homes and commercial buildings.  
404 The results open to the possibility of obtaining 3D surface deformation maps shortly after the  
405 occurrence of large, rapid moving landslides using high resolution SAR data.

406

407 **Key words:** Landslide mapping, emergency scenario, SAR, pixel-offset, surface deformation  
408 monitoring, Montescaglioso, southern Italy.

409

## 410 1. Introduction

411 Large landslides occur in several regions of the Earth, causing damage and casualties (Petley, 2012). In  
412 places, these phenomena affect urban areas, buildings, roads and rails, threatening the population and  
413 causing emergency situations. In such scenarios, rapid mapping of the location and extent of the  
414 surface deformation caused by large landslides can provide important hints for the rapid response of  
415 civil protection authorities, for rescue and recovery operations, and to design and deploy effective  
416 monitoring systems (Giordan et al., 2013). Most commonly, post-event landslide maps are compiled  
417 through field mapping, and/or the visual analysis of aerial photographs taken shortly after a landslide  
418 event (Guzzetti et al., 2012). Where the ground displacements are in the order of several meters, and  
419 the velocity of the failure is rapid to very rapid (Cruden and Varnes, 1996), access to the landslide area  
420 may be difficult or impossible, or too dangerous to perform field mapping. In these circumstances,  
421 remote sensing techniques provide an effective alternative to perform semi-quantitative or quantitative  
422 assessments of the extent and the amount of the ground deformations (Singleton et al., 2014, and  
423 references therein).

424 Among several remote sensing techniques, space-borne Synthetic Aperture Radar (SAR) has  
425 demonstrated its efficiency to monitor changes on the Earth's surface produced by natural and human  
426 induced processes (Rott, 2009). In particular, Differential SAR Interferometry (DInSAR) allows  
427 measuring ground deformation by analysing the phase difference between two SAR images (Massonnet  
428 et al., 1993) acquired over the same area at different times and from different orbital positions  
429 (hereafter referred to as temporal and spatial baselines, respectively). The main advantage of DInSAR  
430 is the possibility to measure sub-centimetre surface displacements over large areas ( $10^2$ - $10^5$  km<sup>2</sup>). For  
431 studying landslides, the application of DInSAR techniques can be limited locally by the unsuitable  
432 exposure of the unstable slopes with respect to the acquisition geometry, and by large and/or rapid  
433 displacements, which may overcome the maximum detectable surface velocities between consecutive  
434 SAR acquisitions (Wasowski and Bovenga, 2014). In the latter case, interferometric phase information  
435 may be affected by high fringe rates leading to processing difficulties in the phase unwrapping step,  
436 and/or to coherence loss due to misregistration errors (Casu et al., 2011). If the deformation introduces  
437 geometric distortions without significantly affecting the SAR image reflectivity, displacements can be  
438 observed in the amplitudes of the SAR image pairs acquired before and after the event, with a method  
439 hereinafter referred to as "pixel-offset" (PO).

440 Compared with standard DInSAR, the PO approach applied to SAR imagery provides 2-D  
441 displacement information i.e., the displacement components across and along the satellite's track  
442 (range and azimuth direction, respectively). Ground displacements that can be detected using the PO  
443 approach are around 1/10 to 1/20 of the pixel size, which for modern SAR sensors is in general in the  
444 order of a few meters. The PO approach provide an additional and complementary tool to analyse and  
445 interpret surface deformations in areas where standard DInSAR techniques are hindered by geometrical  
446 or morphological constrains (e.g., [Manconi and Casu, 2012](#)). Although the PO approach is becoming  
447 popular to monitor ground displacements in unstable slopes ([Gance et al., 2014](#)), the approach has been  
448 so far rarely applied to event landslide scenarios, and in general the majority of the studies have  
449 considered optical imagery ([Singleton et al., 2014](#) and references therein).

450 In this work, we present the first results of a rapid mapping effort conducted during a recent landslide  
451 emergency occurred in 3 December 2013 in the Montescaglioso municipality, Basilicata, southern Italy  
452 ([Fig. 1](#)). In the following, we first describe the main features of the event landslide. We then present  
453 qualitative and semi-quantitative information obtained immediately after the event using consolidated  
454 mapping approaches ([Guzzetti et al., 2012](#)). Next, we show the surface deformation map obtained using  
455 the PO technique applied to high-resolution SAR images acquired by the COSMO-SkyMed (CSK)  
456 satellites before and after the landslide event. PO analyses of SAR images captured along ascending  
457 and descending orbits allowed to retrieved the full three-dimensional deformation field caused by the  
458 landslide ([Raucoules et al., 2013](#); [Hu et al., 2014](#)).

## 459 **2. Local setting**

460 A large landslide struck the SW slope of Montescaglioso, a town located in the Matera Province,  
461 southern Italy, on 3 December 2013, after 56 hours of continuous rainfall ([Fig. 1](#)). As many other  
462 towns in southern Italy, Montescaglioso was built at the top of a hill bounded by steep slopes affected  
463 by multiple landslides of different types ([Cruden and Varnes, 1996](#)). In particular, the slope affected by  
464 the new landslide is characterized by large, deep-seated, ancient slope failures ([Boenzi et al., 1971](#)).  
465 Annual rainfall in the area averages 570 mm, with most of the rainfall falling in November (187 mm).  
466 In the general area crop out sediments of the "Bradanic trough", Pleistocene in age ([Tropeano et al.,](#)  
467 [2002](#)), including a regression (coarsening upward) sequence made up of clay (at the bottom), sand and  
468 gravel (at the top). In the slope affected by the new Montescaglioso landslide, sediments are  
469 heterogeneous, as demonstrated by the presence of large blocks of conglomerates (with a maximum

470 size of about 5 m × 3 m) found at different elevations in the slope. We attribute the chaotic distribution  
471 of the materials to repeated, old and very old landslides; the result of a complex morphological  
472 evolution of the area.

### 473 3. The new Montescaglioso landslide

474 Between 5 and 8 October 2013, the general area between Apulia and Basilicata, including the town of  
475 Montescaglioso, was struck by a severe rainfall event with cumulated rainfall  $E = 246$  mm, and mean  
476 rainfall intensity  $I = 3.6$  mm·h<sup>-1</sup>. The regional rainfall event caused widespread flooding, numerous  
477 shallow landslides, severe economic losses, and four fatalities. A second rainfall event hit the  
478 Montescaglioso area in the period from 30 November, 14:00 CET, to 2 December, 22:00 CET, with a  
479 cumulated rainfall measured at the Ginosa rain gauge, eight kilometers from Montescaglioso, of  $E =$   
480 151.6 mm, and mean rainfall intensity  $I = 2.7$  mm·h<sup>-1</sup>. The two events exceeded 70% of the mean  
481 annual precipitation.

482 The length of the landslide measured along the main displacement axis is  $L_L \sim 1.2 \times 10^3$  m, and the  
483 width measured perpendicularly to the main axis is  $W_L \sim 8.0 \times 10^2$  m, for a total landslide area  $A_L \sim$   
484  $3.0 \times 10^5$  m<sup>2</sup>. The deep-seated slope failure occurred along a SSW facing slope, and extended from ~200  
485 m of elevation in the source area to ~110 m of elevation at the toe, with an average terrain gradient of  
486 ~10%. Movement of the landslide damaged or destructed more than 500 m of the main road connecting  
487 the town of Montescaglioso to the Province Road SP175. The large failure involved a few warehouses,  
488 a supermarket, and private homes located on the right bank of a channel in the area known as “Cinque  
489 Bocche” (Fig. 1). Anecdotal information collected immediately after the event reveals that the  
490 landslide was rapid (Cruden and Varnes, 1996), with the main movement occurring in a short period of  
491 15-20 minutes, corresponding to an estimated average velocity of about 0.5-1 meters/minute. The  
492 movement started at 13:05 CET, and affected the road shortly afterward. Next, the movement involved  
493 the lower-left flank of the landslide, resulting in the formation of a swarm of scarps and counter-scarps,  
494 several tens of meters in length and with a maximum height of seven to eight meters. A house (shown  
495 by “C” in Fig. 1) was moved a few meters downslope and tilted. Fortunately, the building did not  
496 collapse, and allowed the inhabitants to escape avoiding direct consequences.

#### 497 **4. Geomorphological mapping of the new Montescaglioso landslide**

498 To respond to a request of the Italian National Department for Civil Protection (DPC), in the period  
499 from 9 to 24 December 2013, immediately after the landslide, we conducted an initial  
500 geomorphological analysis to prepare a preliminary landslide inventory map, and to characterize the  
501 new Montescaglioso landslide in the context of the pre-existing landslides in the study area. This was  
502 done through the visual interpretation of seven sets of 30 black-and-white stereoscopic aerial  
503 photographs taken from 1947 to 2003, at scales ranging from 1:24,000 to 1:36,000 (**Table S5** in  
504 Supplementary Material). The aerial photographs were obtained as images in JPG format at low  
505 resolution (88 dpi of the negative) from the online catalogue of aerial photographs of the Istituto  
506 Geografico Militare Italiano (IGMI, <http://www.igmi.org/voli/>). The images were printed, and visually  
507 analysed using a mirror “double vision” stereoscope with image magnifications ranging from 1.5× to  
508 15×. Despite the low resolution of the aerial photographs, visual inspection allowed to identify and map  
509 a large number of geomorphological features related to the presence of pre-existing mass movements in  
510 the area. A set of photographical characteristics and morphological features were examined on the  
511 stereoscopic aerial photographs, including shape, size, photographic colour, tone, mottling, texture,  
512 pattern of objects, site topography, and setting (**Guzzetti et al., 2012**). The geomorphological features  
513 were drawn on transparent plastic sheets placed over the aerial photographs, and then digitized  
514 exploiting GIS software and a 2006 digital ortho-photomap available through a WMS service provided  
515 by the Italian Environmental Ministry (<http://www.pcn.minambiente.it>).

516 The geomorphological landslide map shows (**Fig. S1** in Supplementary Material): (i) a large, very old  
517 landslide, largely dismantled by erosion processes, including other landslides, that affected the entire  
518 slope, (ii) a number of smaller and more recent landslides, mainly translational slides and flows, which  
519 are distributed within and at the edges of the pre-existing, very old landslide, and (iii) numerous,  
520 mostly minor, landslide escarpments. Inside the pre-existing, very old landslide we recognized different  
521 generations of landslides. Some of these landslides affect the town of Montescaglioso (**Fig. S1** in  
522 Supplementary Material).

523 In addition to the interpretation of the stereoscopic aerial photographs, we performed field surveys to  
524 evaluate the main consequences of the landslide, and to compile a map of the surface deformations in  
525 the landslide area, aimed at identifying zones within the landslide mass that showed different  
526 kinematics (**Parise, 2003**, and references therein). The field surveys were aided by the visual analysis of

527 post-event terrestrial photographs, and photographs taken during helicopter flights (see [Fig. S2](#) and [Fig.](#)  
528 [S6](#) in Supplementary Material). The geomorphological features mapped in the field and through the  
529 inspection of the terrestrial and the helicopter photographs included single fractures, sets of fractures,  
530 tension cracks, trenches up to six meters in depth or width, and pressure ridges. Many of the  
531 geomorphological features mapped immediately after the landslide event were later destroyed by the  
532 construction of temporary roads.

## 533 **5. Three-dimensional surface deformation from space-borne SAR**

534 The Italian Space Agency (ASI) made available a set of X-band CSK images for the study area. The  
535 dataset consists of 31 images taken along ascending orbits in the period from 30 January 2012 to 18  
536 December 2013, and 12 images taken along descending orbits in the period from 21 March 2012 to 12  
537 December 2013. Both sub-sets included a post-event image.

538 First, we performed a conventional DInSAR analysis exploiting acquisitions taken across the  
539 investigated event, using the approach proposed by [Massonet et al. \(1993\)](#). In addition, we carried out  
540 spectral shift compensation and interferometric fringes filtering ([Burgmann et al., 2000](#)). However, in  
541 the area affected by the new Montescaglioso landslide the conventional DInSAR processing produced  
542 unsatisfactory results, which were primarily attributed to the excessive fringe noise related to the fast-  
543 moving deformation pattern of the landslide ([Fig. S3](#) in Supplementary Material). We note that the  
544 retrieved DInSAR signal is generally very noisy also in areas located near (but outside of) the new  
545 Montescaglioso landslide. We consider this a consequence of the large temporal and/or spatial  
546 baselines that characterize the available CSK image pairs across the landslide event and, in general, the  
547 entire data distribution ([Fig. S4](#) in Supplementary Material).

548 Considering the poor quality of the DInSAR results, we applied the amplitude-based, pixel-offset  
549 technique to the SAR data pairs across the event with the smallest spatial baselines, to reduce the  
550 impact of the spatial decorrelation. In particular, we considered the ascending 16 January 2013 - 18  
551 December 2013, and the descending 10 January 2013 - 12 December 2013 data pairs, characterized by  
552 spatial baselines of 155 m and 40 m, respectively, and covering approximately the same time interval  
553 (336 days and 332 days, respectively). For these data pairs, we exploited AMPCOR, a Fortran routine  
554 based on the Normalized Cross Correlation approach, available in the ROI\_PAC software ([Rosen et al.,](#)  
555 [2004](#)). We considered a matching window of 64×64 pixels, and calculated the PO considering a sparse



556 grid with an under-sampling factor of 4 pixels. We applied a spatial smoothing filter to reduce high-  
557 frequency noise. Readers interested in the details of the PO processing used here are referred to [Casu et](#)  
558 [al. \(2011\)](#).

559 As mentioned already, the PO technique allows identifying with a good spatial resolution areas affected  
560 by large displacements, which are on the order of, or exceed the pixel size e.g., three meters for the  
561 available CSK data. Combining the PO measurements obtained exploiting the CSK ascending and  
562 descending orbits, we determined the three-dimensional deformation pattern caused by the new  
563 Montescaglioso landslide ([Fig. 2](#)). Visual inspection of [Fig. 2](#) reveals that the ground displacements  
564 have a dominant SSW component, with values exceeding 10 meters for large parts of the landslide  
565 deposit, and exceeding locally 20 meters. Significant subsidence values were identified in the areas  
566 experiencing the largest damages, whereas a distinct uplift of up to five meters was detected close to  
567 the accumulation area.

## 568 **6. Discussion and Conclusions**

569 The exploitation of remote sensing data and technologies for the rapid mapping of natural and/or  
570 human induced disasters is becoming a standard practice to support civil protection emergency and  
571 recovery operations ([Boccardo, 2013](#)). This includes analyses of data acquired from different remote  
572 platforms (e.g., ground based systems, manned and unmanned aerial systems, space-borne systems),  
573 and exploiting different types of sensors (e.g., panchromatic, multispectral, hyperspectral, thermal,  
574 LiDAR, radar). For large landslides, selection of the most appropriate mapping and monitoring  
575 technique depends on multiple factors ([Wieczorek and Snyder, 2009](#); [Giordan et al., 2013](#)). After a new  
576 landslide event, rapid evaluation of the area affected by the mass wasting, and measurements of the  
577 associated surface deformations, are of primary interest to design and deploy effective monitoring  
578 networks, and to support early warning systems ~~aimed at ensuring the safety of people, structure and~~  
579 ~~infrastructures~~. Post-event deformation maps can also contribute to improved geomorphological  
580 analyses and geophysical investigations, and prove useful for the evaluation of the residual risk, and for  
581 the selection, the design, and the implementation of mitigation and stabilization measures ([Revellino et](#)  
582 [al., 2010](#)).

583 Most commonly, optical images captured by aerial and satellite sensors before and after a landslide  
584 event are used for first order evaluations of ground displacements in emergency scenarios. However,

585 optical data can only provide qualitative and/or semi quantitative bi-dimensional information, and the  
586 possibility of obtaining optical data of sufficient quality depend on local meteorological conditions.  
587 Frequently, during and immediately following the occurrence of rainfall-induced landslides, cloud  
588 coverage limits the visibility of a landslide area. Airborne LiDAR represents an additional remote  
589 sensing tool to detect and map post-event landslide deformation, and to estimate the volume of the  
590 displaced mass (e.g., [Giordan et al., 2013](#)). However, the acquisition of LiDAR data can be limited by  
591 multiple operational constrains, including the local meteorological conditions, and the costs of the  
592 surveys.

593 Where the setting of the local terrain is suitable for the satellite acquisition geometry ([Colesanti and](#)  
594 [Wasowski, 2006](#)), space-borne SAR is a valid alternative to detect, map and measure surface  
595 deformations caused by active landslides. SAR data can be captured in all weather conditions, during  
596 the day and the night, with a significant advantage over other remote sensing techniques, and chiefly  
597 the techniques based on optical (multispectral) data. Although, conventional DInSAR techniques have  
598 known limitations for detecting and measuring the deformation of rapid moving landslides, [Garcia et](#)  
599 [al. \(2013\)](#) have shown recently that processing of L-Band SAR imagery was capable of detecting and  
600 measuring landslide surface velocities up to one meter per year.

601 We have shown that the amplitude information captured by space-borne SAR images can be exploited  
602 to detect, map, and measure deformations caused by large, rapid-moving landslides. For the purpose,  
603 we exploited the “pixel offset” (PO) technique ([Rosen et al., 2004](#).) using pairs of SAR image  
604 acquired before and after the new Montescaglioso landslide by the CSK satellites, which ensures high  
605 spatial resolution ( $3\text{ m} \times 3\text{ m}$ ) and short revisit times (16 days on average for the available datasets).  
606 We combined the PO results obtained from ascending and descending orbits to retrieve the three-  
607 dimensional geometry of the ground displacements. To our knowledge, this is the first time that this  
608 approach was applied to the rapid mapping of the 3D surface displacement of rapid-moving landslides.  
609 The application of the PO technique to obtain a rapid assessment of the surface displacements after an  
610 event depends on two main factors: (i) the availability of SAR imagery, which is constrained by the  
611 satellite configuration and predefined acquisition plan, and (ii) the PO processing time. For the  
612 Montescaglioso landslide case study, the CSK imagery was made available to us 8 and 15 days after  
613 the landslide event, for the descending and the ascending orbits, respectively. To obtain this result, the  
614 CSK acquisition plan was modified specifically to contribute to the Montescaglioso civil protection

615 emergency scenario. The 3D deformation maps computed exploiting the PO technique were delivered  
616 to the civil protection authorities less than 24 hours after receiving the SAR imagery. Depending on the  
617 area of interest and the acquisition plan, the CSK configuration may provide SAR images with shorter  
618 revisit times. In principle, PO results can be produced and delivered just a few days after an event  
619 landslide.

620 The combination of rapid geomorphological mapping, rapid field mapping, and rapid measurements of  
621 3D deformation proved crucial to support civil protection authorities during the emergency following  
622 the new Montescaglioso landslide. The results of the geomorphological multi-temporal analysis  
623 allowed recognizing the presence of pre-existing landslides of different size, shape, and relative age, and  
624 that affect larger areas than those identified in existing official maps and reports. The field mapping  
625 performed shortly after the event allowed to obtain useful information to better understand the  
626 kinematics of the new landslide, and for the reconstruction of the geometry of the slip surface (Parise,  
627 2003). Two major landslide scarps were identified in the area. A first scarp, located in the middle of  
628 slope in the area where the supermarket was located, formed during the initial phase of movement. A  
629 second scarp, located closer to the divide, generated presumably during a second phase of movement,  
630 as a result of the retrogressive evolution of the landslide. The 3D ground deformation measurements  
631 obtained through the PO analysis detected two main directions of movement associated with (Fig. 3) (i)  
632 the main landslide event (SSW), and (ii) a secondary and smaller event (SSE). Thus, the PO results are  
633 in agreement with the magnitude and the deformation mechanisms recognized and mapped in the field.  
634 The combined interpretation of the results obtained with classical and new methods presented in this  
635 work was essential for the design of the topographic monitoring network installed in the  
636 Montescaglioso area. We expect the results obtained to be useful for the selection and the design of the  
637 mitigation strategies that will be implemented in the landslide area, and in the neighbouring regions.

638 Finally, we note that future integrations of information obtained exploiting classical geomorphological  
639 analyses and SAR images, through DInSAR and/or PO techniques, might open new scenarios for the  
640 analysis of rapid-moving landslides characterized by complex spatial and/or temporal heterogeneities  
641 of the deformation field. We expect that the increasing availability of space-borne, high spatial and/or  
642 temporal resolution SAR images, such as COSMO-SkyMed and TerraSAR-X, and the forthcoming  
643 ALOS PALSAR-2 and Sentinel missions, will enhance the possibility to perform the rapid mapping of

644 large landslides in complex emergency scenarios, and to support civil protection authorities in the  
645 aftermath of catastrophic landslide events.

## 646 **7. Acknowledgements**

647 Research funded by the National Department of Civil Protection (DPC). We are grateful to L. Candela  
648 of the Italian Space Agency (ASI) for making available the COSMO-SkyMed images used in this  
649 study.

## 650 **8. References**

- 651 Allasia, P., Manconi, A., Giordan, D., Baldo, M. and Lollino, G.: ADVICE: A New Approach for  
652 Near-Real-Time Monitoring of Surface Displacements in Landslide Hazard Scenarios, *Sensors*,  
653 13(7), 8285–8302, doi:10.3390/s130708285, 2013.
- 654 Boenzi, F., Radina, B., Ricchetti, G. and Valduga, A.: Note illustrative della Carta Geologica d'Italia  
655 alla scala 1:100.000, Foglio 201 Matera, Serv. Geol. It., 48 pp., 1971.
- 656 Boccoardo, P.: New perspectives in emergency mapping, *Eur. J. Remote Sens.*, 571–582,  
657 doi:10.5721/EuJRS20134633, 2013.
- 658 Bürgmann, R., Rosen, P. A. and Fielding, E. J.: Synthetic Aperture Radar Interferometry to Measure  
659 Earth's Surface Topography and Its Deformation, *Annu. Rev. Earth Planet. Sci.*, 28(1), 169–209,  
660 doi:10.1146/annurev.earth.28.1.169, 2000.
- 661 Casu, F., Manconi, A., Pepe, A. and Lanari, R.: Deformation Time-Series Generation in Areas  
662 Characterized by Large Displacement Dynamics: The SAR Amplitude Pixel-Offset SBAS  
663 Technique, *IEEE Trans. Geosci. Remote Sens.*, 49(7), 2752–2763,  
664 doi:10.1109/TGRS.2010.2104325, 2011.
- 665 Colesanti, C. and Wasowski, J.: Investigating landslides with space-borne Synthetic Aperture Radar  
666 (SAR) interferometry, *Eng. Geol.*, 88 (3–4), 173–199, doi:10.1016/j.enggeo.2006.09.013, 2006.
- 667 Cruden, D. M. and Varnes, D. J.: Landslides Types and Processes, in Turner A.K. & Schuster R.L.  
668 *Landslides: Investigation and Mitigation*, pp. 36–75, National Academy Press, WA., 1996.
- 669 Gance, J., Malet, J.-P., Dewez, T. and Travelletti, J.: Target Detection and Tracking of moving objects  
670 for characterizing landslide displacements from time-lapse terrestrial optical images, *Eng. Geol.*,  
671 172, 26–40, doi:10.1016/j.enggeo.2014.01.003, 2014.

- 672 García-Davalillo, J. C., Herrera, G., Notti, D., Strozzi, T. and Álvarez-Fernández, I.: DInSAR analysis  
673 of ALOS PALSAR images for the assessment of very slow landslides: the Tena Valley case  
674 study, *Landslides*, 11(2), 225–246, doi:10.1007/s10346-012-0379-8, 2014.
- 675 Giordan, D., Allasia, P., Manconi, A., Baldo, M., Santangelo, M., Cardinali, M., Corazza, A.,  
676 Albanese, V., Lollino, G. and Guzzetti, F.: Morphological and kinematic evolution of a large  
677 earthflow: The Montaguto landslide, southern Italy, *Geomorphology*, 187, 61–79,  
678 doi:10.1016/j.geomorph.2012.12.035, 2013.
- 679 Guzzetti, F., Mondini, A. C., Cardinali, M., Fiorucci, F., Santangelo, M. and Chang, K.-T.: Landslide  
680 inventory maps: New tools for an old problem, *Earth Sci. Rev.*, 112, 42–66,  
681 doi:10.1016/j.earscirev.2012.02.001, 2012.
- 682 Hu, J., Li, Z. W., Ding, X. L., Zhu, J. J., Zhang, L. and Sun, Q.: Resolving three-dimensional surface  
683 displacements from InSAR measurements: A review, *Earth-Sci. Rev.*, 133, 1–17,  
684 doi:10.1016/j.earscirev.2014.02.005, 2014.
- 685 Manconi, A. and Casu, F.: Joint analysis of displacement time series retrieved from SAR phase and  
686 amplitude: Impact on the estimation of volcanic source parameters, *Geophys. Res. Lett.*, 39(14),  
687 n/a–n/a, doi:10.1029/2012GL052202, 2012.
- 688 Massonnet, D., Rossi, M., Carmona, C., Adragna, F., Peltzer, G., Feigl, K. and Rabaut, T.: The  
689 displacement field of the Landers earthquake mapped by radar interferometry, *Nature*, 364(6433),  
690 138–142, doi:10.1038/364138a0, 1993.
- 691 Parise, M.: Observation of surface features on an active landslide, and implications for understanding  
692 its history of movement, *Nat Hazards Earth Syst Sci*, 3(6), 569–580, doi:10.5194/nhess-3-569-  
693 2003, 2003.
- 694 Petley, D.: Global patterns of loss of life from landslides, *Geology*, 40(10), 927–930,  
695 doi:10.1130/G33217.1, 2012.
- 696 Raucoules, D., de Michele, M., Malet, J.-P. and Ulrich, P.: Time-variable 3D ground displacements  
697 from high-resolution synthetic aperture radar (SAR). Application to La Valette landslide (South  
698 French Alps), *Remote Sens. Environ.*, 139, 198–204, doi:10.1016/j.rse.2013.08.006, 2013.
- 699 Revellino, P., Grelle, G., Donnarumma, A. and Guadagno, F. M.: Structurally controlled earth flows of  
700 the Benevento province (Southern Italy), *Bull. Eng. Geol. Environ.*, 69(3), 487–500,  
701 doi:10.1007/s10064-010-0288-9, 2010.

- 702 Rosen, P. A., Hensley, S., Peltzer, G. and Simons, M.: Updated repeat orbit interferometry package  
703 released, *Eos Trans. Am. Geophys. Union*, 85(5), 47–47, doi:10.1029/2004EO050004, 2004.
- 704 Rott, H.: Advances in interferometric synthetic aperture radar (InSAR) in earth system science, *Prog.*  
705 *Phys. Geogr.*, 33(6), 769–791, doi:10.1177/0309133309350263, 2009.
- 706 Singleton, A., Li, Z., Hoey, T. and Muller, J.-P.: Evaluating sub-pixel offset techniques as an  
707 alternative to D-InSAR for monitoring episodic landslide movements in vegetated terrain,  
708 *Remote Sens. Environ.*, 147, 133–144, doi:10.1016/j.rse.2014.03.003, 2014.
- 709 Tropeano, M., Sabato, L. and Pieri, P.: Filling and cannibalization of a foredeep: the Bradanic Trough,  
710 Southern Italy, *Geol. Soc. Lond. Spec. Publ.*, 191, 55–79, doi:10.1144/GSL.SP.2002.191.01.05,  
711 2002.
- 712 Wasowski, J. and Bovenga, F.: Investigating landslides and unstable slopes with satellite Multi  
713 Temporal Interferometry: Current issues and future perspectives, *Eng. Geol.*, 174, 103–138,  
714 doi:10.1016/j.enggeo.2014.03.003, 2014.
- 715 Wieczorek, G. F. and Snyder, J. B.: Monitoring slope movements, *Geol. Monit.*, 245–271, 2009.  
716  
717

718 **Figures**

719 **Figure 1.** Montescaglioso, southern Italy. The red area shows the approximate area affected by the 3  
720 December 2013 Montescaglioso landslide. Location of a supermarket (A), and of most damaged  
721 buildings (B and C) is shown. (D) and (E) show locations of the Cinque Bocche and Capoiazzo  
722 channels. Source of terrain map: Google Earth™.

723



724

725

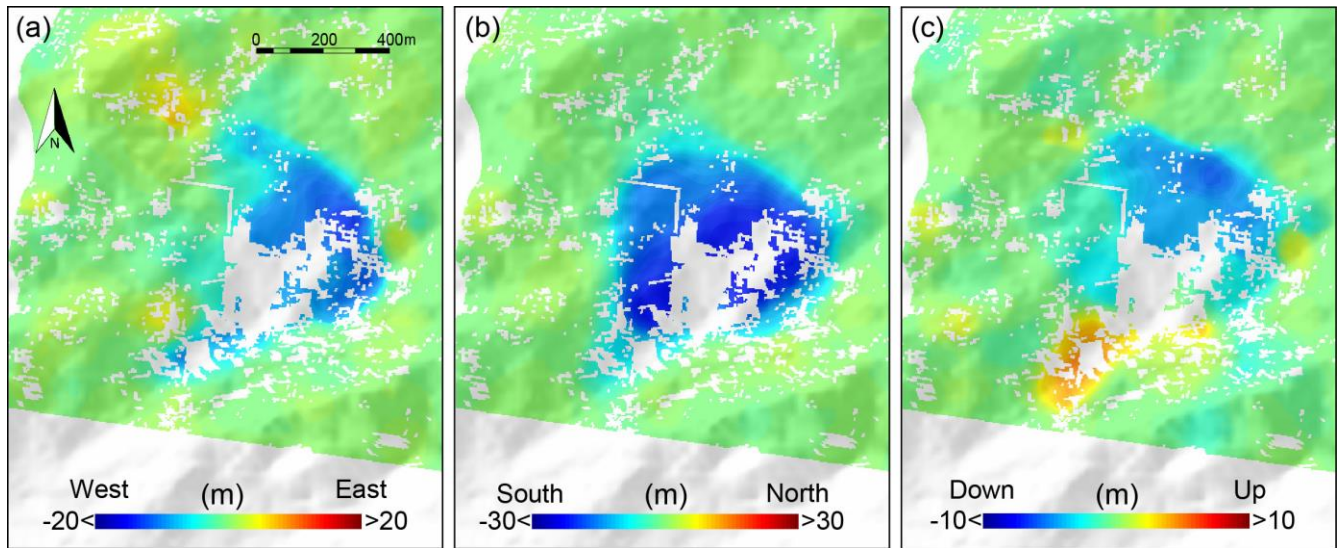
726

727



728 **Figure 2.** The new Montescaglioso landslide of 3 December 2013. Pixel-offset results for the (a) East-  
 729 West, (b) North-South, and (c) Up-Down components of the surface deformation. Measurements are  
 730 the results of the combination of pixel-offset results obtained processing COSMO-SkyMed images  
 731 acquired along ascending and descending orbits.

732



733

734

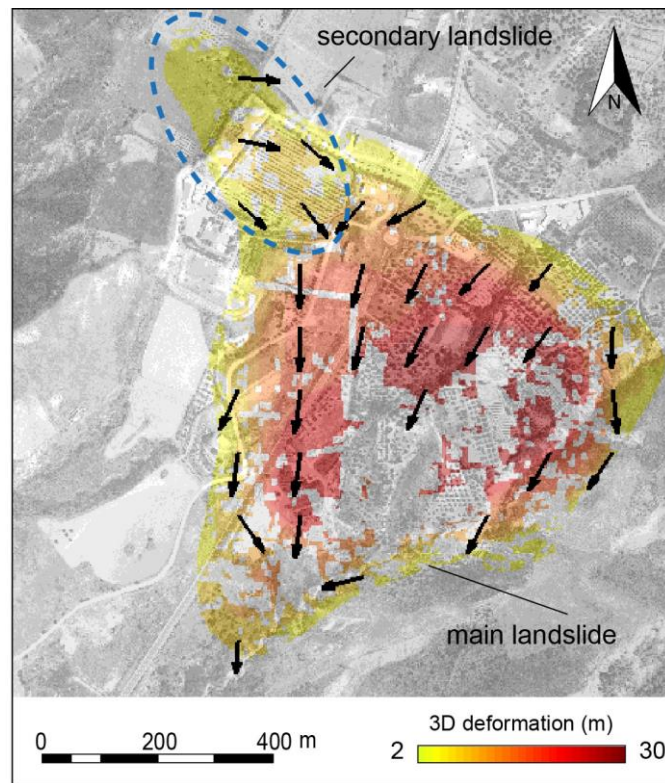
735

736



737 **Figure 3.** The new Montescaglioso landslide of 3 December 2013. Map of the surface deformation  
738 obtained through the Pixel-Offset (PO) analysis prepared using the ©3DA approach (Allasia et al.,  
739 2013). Colours show magnitude of the 3D deformation field. Arrows show direction of movement (unit  
740 vectors) derived from the PO analysis in the EW-NS plane. Deformations smaller than two meters are  
741 not shown. The deformation field shows two main directions of motion: (i) a dominant SSW direction  
742 caused by the main landslide, and (ii) a secondary SSE direction caused by a parasitic landslide,  
743 encompassed by the dashed blue ellipse.

744



745

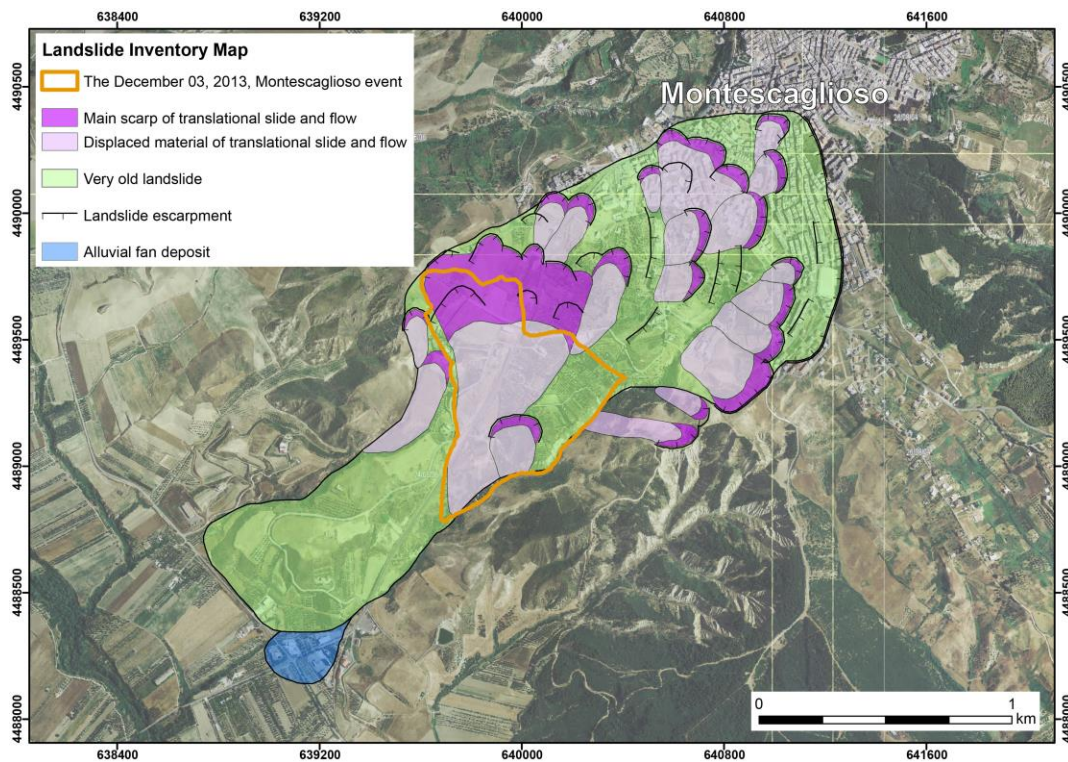
746

747 **Supplementary Material of the Manuscript**

748

749 **S1.** Landslide inventory map realized along the SW slope of the hill where is located the  
750 Montescaglioso village. The map is carried out by the photointerpretation of different sets of  
751 stereoscopic aerial photographs taken in the period 1947-2003. The map shows: (i) a very old landslide  
752 (light green in the map); (ii) slide, slide flows and flows (violet in the map) distributed inside and at the  
753 boundary of the very old landslide; (iii) main landslide escarpments and (iv) alluvial fan deposit (light  
754 blue in the map). Superimposed to the pre-existing landslides, in orange is represented the 3 December  
755 2013, Montescaglioso landslide. The base map is the WMS 2006 color orto-photomap, downloaded  
756 from <http://www.pcn.minambiente.it>.

757



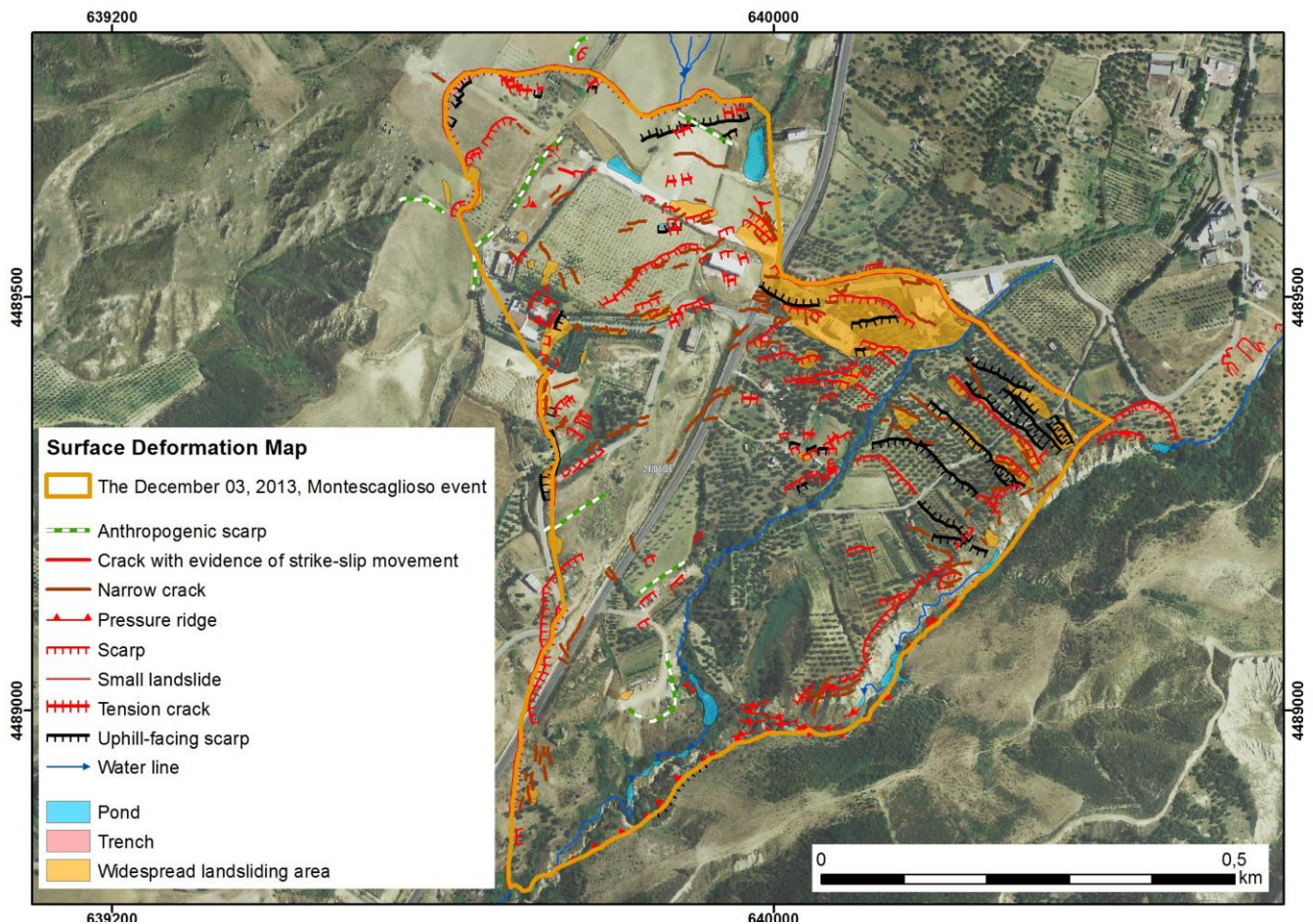
758

759



760 **S2.** High resolution map of the surface deformation produced by the new Montescaglioso landslide, as  
 761 identified by field surveys. The moving mass determined the formation of pressure ridges and thrusts  
 762 for some hundreds of meters, as well as the damming of Fosso Capoiazzo, with consequent formation  
 763 of several lakes. In particular, the area of the original confluence between the two water lines (Canale  
 764 Cinque Bocche and Fosso Capoiazzo, see also Fig. 1) was considerably modified, being strongly  
 765 altered the hydrographic network due to the accumulation of the material pushed from upstream. A  
 766 further lake was formed at this site, too. The morphological characters observed and mapped indicate  
 767 that the phenomenon was a translational slide, with main direction of movement towards SW. In its  
 768 middle-lower portion, because of the obstacle constituted by the body of an ancient paleo-landslide  
 769 delimited by the two water lines mentioned above, the direction of the main movement changed toward  
 770 SSW, strongly conditioned by the right flank of the landslide, approximately striking NS. The base map  
 771 is the WMS 2006 color orto-photomap, downloaded from <http://www.pcn.minambiente.it>.

772

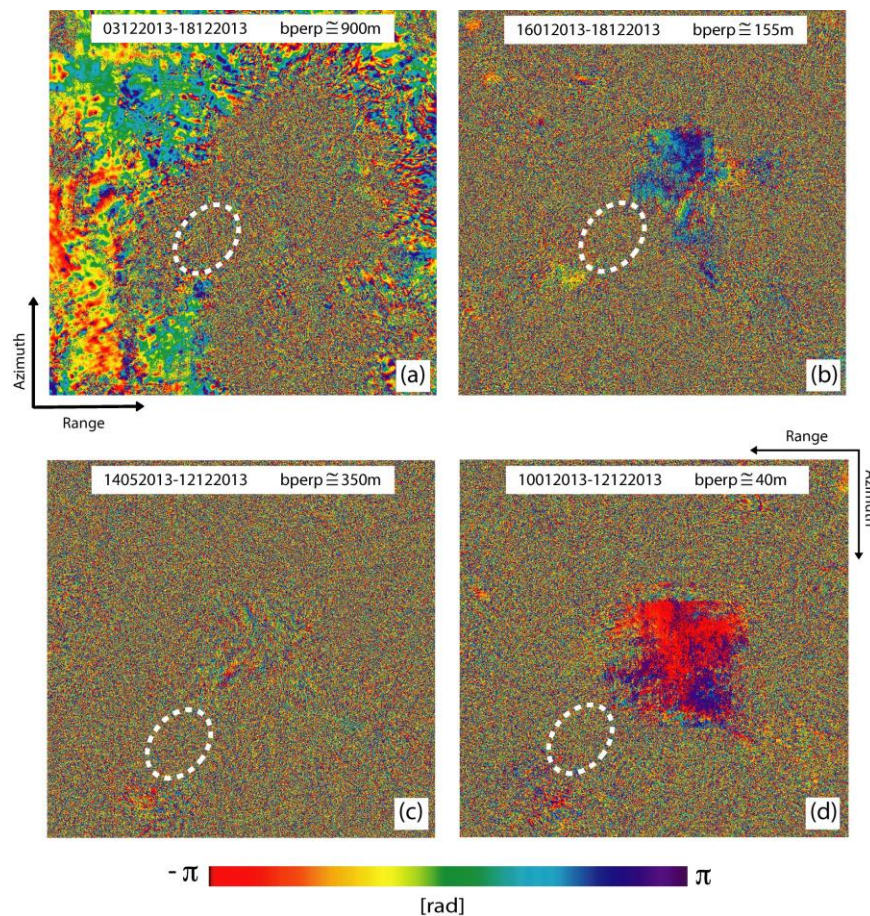


773  
774

775

776 **S3.** DInSAR interferograms relevant to the Montescaglioso landslide area, achieved by exploiting pre-  
 777 and post-event CSK acquisitions over ascending (a-b) and descending (c-d) orbits. (a) 3 December  
 778 2013-18 December 2014 interferogram with perpendicular baseline of about 900 m. (b) 16 January  
 779 2013-18 December 2014 interferogram, 155 m of perpendicular baseline. (c) 14 May 2013-12  
 780 December 2014 interferogram with perpendicular baseline of 350 m. (d) 10 January 2013-12 December  
 781 2014 interferogram, 40 m of perpendicular baseline. The spatial coherence is not preserved due to the  
 782 amount of surface displacements, resulting in the complete loss of coherence of the DInSAR signal in  
 783 the areas experiencing the largest deformations. Note also that the loss of coherence in the area near  
 784 (but outside) the landslide (highlighted by the dashed white ellipse) is generally due to the large  
 785 temporal and/or spatial baseline values characterizing the available SAR data pairs across the event.

786



787

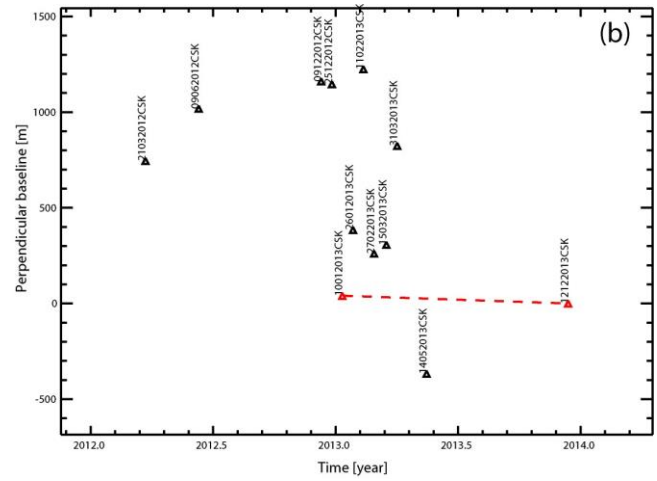
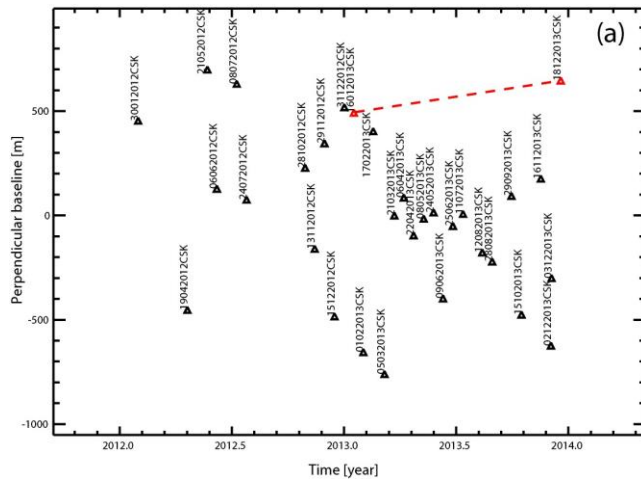
788



789 **S4.** SAR data representation in the temporal/perpendicular baseline plane for the (a) ascending and (b)  
 790 descending CSK datasets. Dates are in the DDMMYYYY format. The black triangles identify the  
 791 whole CSK acquisitions, while the red ones, connected with the dashed red lines, correspond to the  
 792 SAR data pairs used for applying the Pixel Offset technique.

793

794



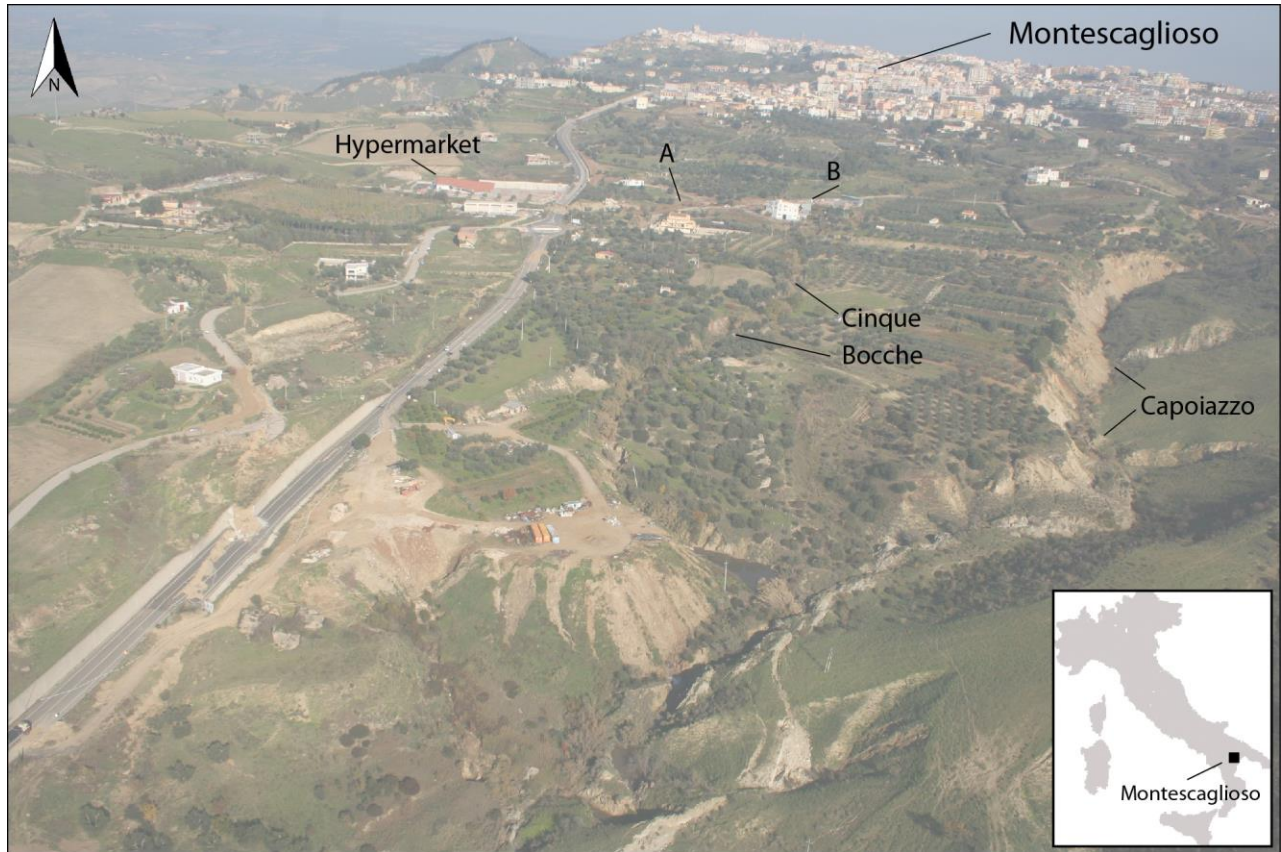
795  
796

797 **S5** Stereoscopic aerial photographs used to prepare the landslide inventory map of the Montescaglioso  
798 study area. The images are available at the website of the Istituto Geografico Militare Italiano (IGMI)  
799 (<http://www.igmi.org/voli/>).

YEAR	STRIP	PHOTOGRAPH	TYPE	SCALE
1947	6	45c, 46c, 47c, 48c, 49c, 45s, 46s, 47s, 48s, 49s	black-and-white	1:24,000
1954	152	6950, 6951, 6952	black-and-white	1:34,000
1972	3bis	5522, 5523, 5524	black-and-white	1:30,000
1989	36	44, 45, 46	black-and-white	1:27,000
1990	31	731, 732, 733	black-and-white	1:36,000
1996	38	90, 91, 92, 93	black-and-white	1:34,000
2003	131	6107, 6108, 6109, 6110	black-and-white	1:30,000
2003	126	6157, 6158, 6159	black-and-white	1:30,000

800  
801

802 **S6.** Aerial photograph taken form helicopter after the landslide. The location of the Hypermarket, as  
 803 well as of the most damaged buildings (A and B) is also identified.  
 804



805

806